

Codimension-Two Bifurcation of a Fractional-Order Schnakenberg Chemical Reaction System

Muhammad Asif Khan^{a,*}, Qamar Din^b, Walid
Abdelfattah^c

^a*Department of Mathematics, Kahuta-Haveli Campus, University of
Poonch Rawalakot, Azad Jammu and Kashmir, Pakistan*

^b*Department of Mathematics, University of Poonch Rawalakot, Azad
Jammu and Kashmir, Pakistan*

^c*Department of Mathematics, College of Arts and Science, Northern
Border University, Saudi Arabia*

asif31182@gmail.com, qamar.sms@gmail.com,

walid.abdelfattah@nbu.edu.sa

(Received August 21, 2024)

Abstract

This article explores the dynamic behavior of a fractional-order Schnakenberg chemical reaction model. Specifically, we conduct an analysis of codimension-two bifurcation associated with 1:2, 1:3, and 1:4 resonances. To achieve these results, we utilize the normal form method and bifurcation theory. The findings are illustrated through detailed numerical simulations, including visualizations like two-parameter bifurcation diagrams and maximum Lyapunov exponent plots. These simulations effectively explore the system's behavior under the influence of two varying parameters within a three-dimensional space. Additionally, the simulations vividly demonstrate the theoretical results and offer valuable insights into the underlying dynamics.

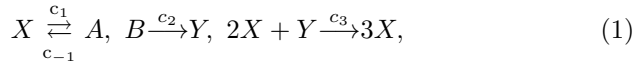
*Corresponding author.

1 Introduction

Nature is full of cyclical and oscillatory processes, with circadian rhythms found in nearly every aspect of life being perhaps the most recognized of these repetitive phenomena. In 1979, J. Schnakenberg developed a device that exhibited sustained oscillations in a simple glycolysis model [1], which bore a striking resemblance to a system of four reactions known as the Brusselator [2]. Schnakenberg-type systems are widely applicable, particularly in analyzing skin and in the pattern formation processes during embryogenesis [3,4]. A study explored a chemical Schnakenberg model [5], illustrating autochemical processes with rhythmic behavior that could have diverse biological and biochemical applications. Considering feedback control, Noufaey [6] explored semi-analytical solutions for the Schnakenberg system within a reaction–diffusion cell. Numerical solutions for a variable-order space-time fractional reaction-diffusion Schnakenberg model were examined in [7]. Sattari and Tuomela [8] explored the numerical simulation of the Schnakenberg system, with a focus on the dynamics of an evolving surface. In [9], authors investigated the transient behavior of the Schnakenberg model within the context of reaction–diffusionadvection processes. In [10], the authors examined the formation of Turing patterns in a Schnakenberg-type model, considering the effects of both diffusion and delay. Liu and Wang [11] investigated the pattern formation in the Schnakenberg model with a coupled two-cell system. In [12], the authors conducted a bifurcation analysis of the reaction–diffusion Schnakenberg system. In [13], the authors considered the reaction–diffusion Schnakenberg system for numerical solutions. Ishii and Kurata [14] developed symmetric one-peak stationary solutions for the Schnakenberg model in the presence of heterogeneity. Jasim and Rana [27] studied a codimension one bifurcations and chaos control of discrete-time fractional order Schnakenberg model. For further studies related to different classes of the Schnakenberg model, see [15–19] and the references cited therein.

The Schnakenberg model is among the simplest reaction kinetic models, originating from a series of hypothetical tri-molecular autocatalytic reactions proposed by Schnakenberg [1]. This model was created to identify the

minimal number of reactions and reactants needed to exhibit limit-cycle behavior. Schnakenberg demonstrated that a minimum of three reactions, with at least one being autocatalytic, is necessary for this type of model. Thus, the following reaction scheme is obtained for the general chemicals A, X, Y and B :



where A and B are chemicals with constant concentrations. Applying the law of mass action, we obtain the following differential equations:

$$\begin{cases} \frac{dU_X}{d\tau} = c_1 U_A - c_{-1} U_X + c_3 U_X^2 U_Y, \\ \frac{dU_Y}{d\tau} = c_2 U_B - c_3 U_X^2 U_Y, \end{cases} \quad (2)$$

where $U_A, U_B, U_X,$ and U_Y represent the quantities of $A, B, X,$ and Y molecules in the reaction vessel, respectively. To nondimensionalize system (2), we define the variables and parameters as follows: $x = \sqrt{\frac{c_3}{c_{-1}}} U_X, y = \sqrt{\frac{c_3}{c_{-1}}} U_Y, a = \frac{c_1}{c_{-1}} \sqrt{\frac{c_3}{c_{-1}}} U_A, b = \sqrt{\frac{c_2}{c_{-1}}} U_B,$ and $t = k_{-1} \tau$. Consequently, the system transforms accordingly:

$$\begin{cases} \frac{dx}{dt} = a + x^2 y - x, \\ \frac{dy}{dt} = b - x^2 y. \end{cases} \quad (3)$$

Unlike conventional integer-order models, fractional-order models include fractional derivatives in their equations. This approach can offer a more precise depiction of reaction kinetics. These models are employed to gain deeper insights into the fundamental mechanisms of chemical reactions, enhance chemical processes, and create innovative materials and technologies. They are also utilized in medical applications to simulate drug delivery systems and analyze physiological processes. In summary, fractional-order chemical reaction models are a valuable tool in chemistry and related fields [24].

Taking into account the facts that fractional calculus provides more accurate modeling of complex systems that cannot be captured by integer-order differential equations, and that fractional systems can be tailored to

fit a wide range of data sets, it is more suitable to examine the fractional-order counterpart of system(3):

$$\begin{cases} x_{n+1} = x_n + \frac{s^m}{\Gamma(m+1)} (a + x_n^2 y_n - x_n), \\ y_{n+1} = y_n + \frac{s^m}{\Gamma(m+1)} (b - x_n^2 y_n). \end{cases} \quad (4)$$

where $0 < m \leq 1$ is fractional derivative of order m , and $s > 0$ denotes the step size used for discretization.

Recently, Khan and Din [23] studied a discrete-time fractional order chemical reaction system and explore stability, codimension one and codimension-two bifurcations. In [2], the Brusselator system is discretized using the Euler approximation to investigate flip and Hopf bifurcations and a new exponential-type chaos control method is proposed for the discrete-time Brusselator system. In [20], the stability, bifurcation, and chaos control of two discrete classes of the glycolysis system are analyzed. Din et al. [21] applied the Euler approximation and a nonstandard finite difference scheme to discretize a chemical reaction system. Din and Asad [22] studied period-doubling bifurcation, Neimark-Sacker bifurcation and chaos control in a discretized enzyme model by employing the Euler forward approximation. Din and Haider [25] studied the Hopf bifurcation of system (3) and showed that its discrete-time counterpart, obtained via the Euler approximation, undergoes a Neimark-Sacker bifurcation as well as a period-doubling bifurcation. To maintain the dynamical consistency of continuous models, a nonstandard finite difference scheme is proposed for the Schnakenberg model (3). It is proven that the continuous system undergoes a Hopf bifurcation at its interior equilibrium, while the discrete-time system, using the nonstandard finite difference scheme, undergoes a Neimark-Sacker bifurcation at its interior fixed point. Recently, Din [26] studied codimension-one and codimension-two bifurcations for a discrete fractional-order Brusselator model. For more information on mathematical models related to the chemical reaction dynamics and bifurcations of fractional-order systems, readers are encouraged to consult references [29–37].

The novel contributions of this paper are outlined as follows:

- The study explores multi-parameter bifurcation phenomena in the context of a discrete-time fractional order Schnakenberg model. Investigating the 1:2, 1:3, and 1:4 strong resonance conditions reveals intricate and non-trivial dynamics, such as limit cycles and chaos, offering a deeper understanding of how the Schnakenberg model behaves under these specific resonance states.
- Understanding how fractional order discrete dynamics impact the Schnakenberg model is a novelty in itself. By discretizing the continuous-time model, researchers can gain insights into how fractional order discrete time steps influence the system's stability and behavior, which is crucial for comprehending real-world biochemical processes with inherent discrete nature.
- Studying the coexistence of different resonance regimes provides valuable insights into the robustness and sensitivity of the fractional order Schnakenberg model under varying parameter values. This knowledge is essential in understanding how the pathway responds to changes in the environment and internal conditions.
- The research bridges the gap between the fields of nonlinear dynamics, mathematical biology, and biochemical engineering. The insights gained from studying discrete-time fractional order models have implications beyond the specific pathway, potentially benefiting other areas of research involving dynamical systems and complex networks.

The rest of this paper is structured as follows:

Stability analysis of system (4) is discussed in Section 2. Codimension-two bifurcations (that is, 1:2, 1:3 and 1:4 strong resonances) are studied in Section 3 and in Section 4 numerical simulations are presented.

2 Stability analysis

It is easy to see that system Eq. (4) has unique positive fixed point $E(x_*, y_*) = (a + b, \frac{b}{(a+b)^2})$.

Subsequently, we examine the local stability analysis of $E(x_*, y_*) = (a + b, \frac{b}{(a+b)^2})$ of system Eq. (4).

To investigate the stability, we compute the Jacobian matrix F_J of system (4) at $E(x_*, y_*)$ as follow:

$$F_J(E) = \begin{pmatrix} \frac{(b-a)s^m}{(a+b)\Gamma(m+1)} + 1 & \frac{(a+b)^2 s^m}{\Gamma(m+1)} \\ -\frac{2bs^m}{(a+b)\Gamma(m+1)} & 1 - \frac{(a+b)^2 s^m}{\Gamma(m+1)} \end{pmatrix}.$$

The characteristic polynomial of F_J at $E(x_*, y_*)$ is given by:

$$\mathbb{F}(\varsigma) = \varsigma^2 - \tau_1(E)\varsigma + \tau_2(E), \tag{5}$$

where

$$\tau_1(E) = -\frac{(a + b)^2 s^m}{\Gamma(m + 1)} + \frac{(b - a)s^m}{(a + b)\Gamma(m + 1)} + 2,$$

and

$$\tau_2(E) = \frac{s^m ((a + b)^3 s^m - (a^3 + 3a^2b + 3ab^2 + a + b^3 - b) \Gamma(m + 1))}{(a + b)\Gamma(m + 1)^2} + 1.$$

The following Lemma is used to explore the stability of fixed point.

Lemma 1. *Let $\mathbb{F}(\varsigma) = \varsigma^2 - \tau_1(E)\varsigma + \tau_2(E)$, and $\mathbb{F}(1) > 0$. Moreover, ς_1, ς_2 are root of \mathbb{F} , then:*

- (i) $|\varsigma_1| < 1$ and $|\varsigma_2| < 1$ if and only if $\mathbb{F}(-1) > 0$ and $\tau_2(E) < 1$;
- (ii) $|\varsigma_1| < 1$ and $|\varsigma_2| > 1$ or $|\varsigma_1| > 1$ and $|\varsigma_2| < 1$ if and only if $\mathbb{F}(-1) < 0$;
- (iii) $|\varsigma_1| > 1$ and $|\varsigma_2| > 1$ if and only if $\mathbb{F}(-1) > 0$ and $\tau_2(E) > 1$;
- (iv) $\varsigma_1 = -1$ and $\varsigma_2 = -1$ if and only if $\tau_1(E) = -2$ and $\tau_2(E) = 1$;
- (v) ς_1 and ς_2 are complex and $\varsigma_{1,2} = -\frac{1}{2} \pm i\frac{\sqrt{3}}{2}$ if and only if $\tau_1(E) = -1$ and $\tau_2(E) = 1$;
- (vi) ς_1 and ς_2 are complex and $\varsigma_{1,2} = \pm i$ if and only if $\tau_1(E) = 0$ and $\tau_2(E) = 1$;

As ς_1 and ς_2 are eigenvalue of (5), we have the following Topological type results. The fixed point $E(x_*, y_*)$ is known as sink if $|\varsigma_1| < 1$ and $|\varsigma_2| < 1$ thus the sink is locally asymptotic stable. The fixed point $E(x_*, y_*)$ is known as source if $|\varsigma_1| > 1$ and $|\varsigma_2| > 1$, thus source is always unstable.

The fixed point $E(x_*, y_*)$ is known as saddle point if $|\varsigma_1| < 1$ and $|\varsigma_2| > 1$ or ($|\varsigma_1| > 1$ and $|\varsigma_2| < 1$) and the fixed point $E(x_*, y_*)$ is known as non-hyperbolic fixed point either $|\varsigma_1| = 1$ and $|\varsigma_2| = 1$.

Thus, by applying Lemma 1, we study the local stability of positive equilibrium point of system (4) by stating the following proposition.

Proposition 1. *The positive equilibrium point $E(x_*, y_*)$ of system (4) satisfies the following results.*

(i) The positive fixed point $E(x_*, y_*)$ is sink if and only if:

$$\frac{s^m \left((a+b)^3 s^m - 2(a^3 + 3a^2b + 3ab^2 + a + b^3 - b) \Gamma(m+1) \right)}{(a+b)\Gamma(m+1)^2} + 4 > 0,$$

and

$$s^m \left((a+b)^3 s^m - (a^3 + 3a^2b + 3ab^2 + a + b^3 - b) \Gamma(m+1) \right) < 0.$$

(ii) The positive fixed point $E(x_*, y_*)$ is saddle point if and only if:

$$\frac{s^m \left((a+b)^3 s^m - 2(a^3 + 3a^2b + 3ab^2 + a + b^3 - b) \Gamma(m+1) \right)}{(a+b)\Gamma(m+1)^2} + 4 < 0.$$

(iii) The positive fixed point $E(x_*, y_*)$ is source if and only if:

$$\frac{s^m \left((a+b)^3 s^m - 2(a^3 + 3a^2b + 3ab^2 + a + b^3 - b) \Gamma(m+1) \right)}{(a+b)\Gamma(m+1)^2} + 4 > 0,$$

and

$$s^m \left((a+b)^3 s^m - (a^3 + 3a^2b + 3ab^2 + a + b^3 - b) \Gamma(m+1) \right) > 0.$$

(iv) The positive fixed point $E(x_*, y_*)$ is non-hyperbolic if and only if:

$$\begin{cases} a = s^{-3m}\Gamma(m+1) (s^{2m} + 4s^m\Gamma(m+1) - 4\Gamma(m+1)^2), \\ b = s^{-3m}\Gamma(m+1) (s^m - 2\Gamma(m+1))^2. \end{cases} \quad (6)$$

or

$$\begin{cases} a = \frac{1}{2}\sqrt{3}s^{-3m}\Gamma(m+1)(s^{2m} + 3s^m\Gamma(m+1) - 3\Gamma(m+1)^2), \\ b = \frac{-9\sqrt{3}s^{-3m}\Gamma(m+1)^5 + 18\sqrt{3}s^{-2m}\Gamma(m+1)^4 - 9\sqrt{3}s^{-m}\Gamma(m+1)^3 + \sqrt{3}s^m\Gamma(m+1)}{2(s^{2m} + 3s^m\Gamma(m+1) - 3\Gamma(m+1)^2)}. \end{cases} \tag{7}$$

or

$$\begin{cases} a = \frac{s^{-3m}\Gamma(m+1)(s^{2m} + 2s^m\Gamma(m+1) - 2\Gamma(m+1)^2)}{\sqrt{2}}, \\ b = \frac{-4\sqrt{2}s^{-3m}\Gamma(m+1)^5 + 8\sqrt{2}s^{-2m}\Gamma(m+1)^4 - 4\sqrt{2}s^{-m}\Gamma(m+1)^3 + \sqrt{2}s^m\Gamma(m+1)}{2(s^{2m} + 2s^m\Gamma(m+1) - 2\Gamma(m+1)^2)}. \end{cases} \tag{8}$$

3 Codimension-two bifurcations

In this section, we study the codimension-two bifurcation. It is easy to see that system (4) has a unique positive equilibrium point $(x_*, y_*) = (a + b, \frac{b}{(a+b)^2})$. For an in-depth examination of local stability, co-dimension-1 bifurcation, and chaos control of (4), refer to [27]. In particular, we investigate the existence of 1:2, 1:3 and 1:4 resonances by implementing normal form theory and theory of bifurcation. The following curves identify the occurrence of these resonance points:

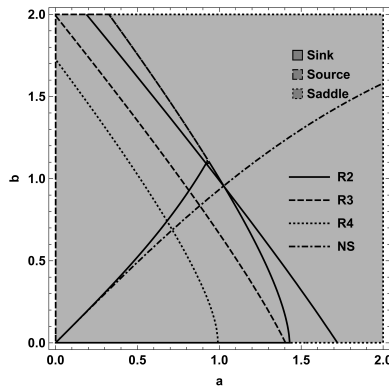


Figure 1. Topological classification for system (4).

$$R2 : \frac{(b-a)s^m}{(a+b)\Gamma(m+1)} - \frac{(a+b)^2 s^m}{\Gamma(m+1)} = -4,$$

$$R3 : \frac{(b-a)s^m}{(a+b)\Gamma(m+1)} - \frac{(a+b)^2 s^m}{\Gamma(m+1)} = -3,$$

$$R4 : \frac{(b-a)s^m}{(a+b)\Gamma(m+1)} - \frac{(a+b)^2 s^m}{\Gamma(m+1)} = -2,$$

and

$$NS : s^m ((a+b)^3 s^m - (a^3 + 3a^2b + 3ab^2 + a + b^3 - b) \Gamma(m+1)) = 0.$$

Then, it is easy to observe that $NS \cap R_2$, $NS \cap R_3$ and $NS \cap R_4$ are known as 1:2, 1:3 and 1:4 resonance points, respectively. Moreover, for $m = 0.577$, $s = 0.789$, $a \in [0.001, 2]$, $b \in [0.001, 2]$, the topological classification for system (4) is shown in Figure 1.

3.1 1:2 strong resonance

This subsection deals with the investigation of 1:2 strong resonance for system (4) at its positive equilibrium point. For this, a and b are chosen to be bifurcation parameters. The Jacobian matrix of system (4) computed at positive equilibrium has eigenvalue -1 with multiplicity two if the following conditions holds true:

$$\begin{cases} \frac{(b-a)s^m}{(a+b)\Gamma(m+1)} - \frac{(a+b)^2 s^m}{\Gamma(m+1)} = -4 \\ s^m ((a+b)^3 s^m - (a^3 + 3a^2b + 3ab^2 + a + b^3 - b) \Gamma(m+1)) = 0. \end{cases} \quad (9)$$

Solving system (9) for h and a yields the following solution (a_0, b_0) :

$$a_0 = s^{-3m} \Gamma(m+1) (s^{2m} + 4s^m \Gamma(m+1) - 4\Gamma(m+1)^2),$$

and

$$b_0 = s^{-3m} \Gamma(m+1) (s^m - 2\Gamma(m+1))^2.$$

Let $x_n = u_n + (a+b)$, $y_n = v_n + \frac{b}{(a+b)^2}$, $a = a_0 + \bar{a}$ and $b = b_0 + \bar{b}$,

then the system (4) can be transformed as follows:

$$\begin{pmatrix} u \\ v \end{pmatrix} \rightarrow \begin{pmatrix} 1 + \mu_{11} & -\mu_{12} \\ \mu_{21} & 1 + \mu_{22} \end{pmatrix} \begin{pmatrix} u \\ v \end{pmatrix} + \begin{pmatrix} f_1(u, v) \\ f_2(u, v) \end{pmatrix}, \quad (10)$$

where $\bar{a} \ll 1$ and $\bar{b} \ll 1$ are small perturbations,

$$\begin{aligned} f_1(u, v) &= \mu_{13}uv + \mu_{14}u^2 + O((|u| + |v|)^3), \\ f_2(u, v) &= \mu_{23}uv + \mu_{24}u^2 + O((|u| + |v|)^3). \end{aligned}$$

$$\mu_{11} = \frac{(b-a)s^m}{(a+b)\Gamma(m+1)}, \quad \mu_{12} = -\frac{(a+b)^2s^m}{\Gamma(m+1)}, \quad \mu_{21} = -\frac{2bs^m}{(a+b)\Gamma(m+1)},$$

$$\mu_{22} = -\frac{(a+b)^2s^m}{\Gamma(m+1)}, \quad \mu_{13} = \frac{2(a+b)s^m}{\Gamma(m+1)}, \quad \mu_{23} = -\frac{2(a+b)s^m}{\Gamma(m+1)},$$

$$\mu_{14} = \frac{bs^m}{(a+b)^2\Gamma(m+1)}, \quad \mu_{24} = -\frac{bs^m}{(a+b)^2\Gamma(m+1)}.$$

Next, we consider the following transformation:

$$\begin{pmatrix} u \\ v \end{pmatrix} = T \begin{pmatrix} w \\ z \end{pmatrix}, \quad (11)$$

where T is a nonsingular matrix given by

$$T = \begin{pmatrix} \frac{\mu_{12}}{\mu_{11}+2} & \frac{\mu_{12}}{(\mu_{11}+2)^2} \\ 1 & 0 \end{pmatrix}.$$

From (10) and (11), it follows that:

$$\begin{pmatrix} w \\ z \end{pmatrix} \rightarrow \begin{pmatrix} P_{10}(a, b) - 1 & P_{01}(a, b) + 1 \\ Q_{10}(a, b) & Q_{01}(a, b) - 1 \end{pmatrix} \begin{pmatrix} w \\ z \end{pmatrix} + \begin{pmatrix} f_3(w, z, a, b) \\ f_4(w, z, a, b) \end{pmatrix}, \quad (12)$$

where

$$f_3(w, z) = P_{20}w^2 + P_{11}wz + P_{02}z^2, \quad f_4(w, z) = Q_{20}w^2 + Q_{11}wz + Q_{02}z^2,$$

$$P_{10} = \frac{\mu_{12}\mu_{21}}{\mu_{11} + 2} + \mu_{22} + 2, \quad P_{01} = \frac{\mu_{12}\mu_{21}}{(\mu_{11} + 2)^2} - 1,$$

$$P_{20} = \frac{\mu_{12}((\mu_{11} + 2)\mu_{23} + \mu_{12}\mu_{24})}{(\mu_{11} + 2)^2},$$

$$P_{11} = \frac{\mu_{12}((\mu_{11} + 2)\mu_{23} + 2\mu_{12}\mu_{24})}{(\mu_{11} + 2)^3}, \quad P_{02} = \frac{\mu_{12}^2\mu_{24}}{(\mu_{11} + 2)^4},$$

$$Q_{20} = \left(\mu_{14} - \mu_{23} - \frac{\mu_{12}\mu_{24}}{\mu_{11} + 2} \right) \mu_{12} + (\mu_{11} + 2)\mu_{13},$$

$$Q_{11} = \frac{\mu_{13}(\mu_{11} + 2)^2 + \mu_{12}((\mu_{11} + 2)(2\mu_{14} - \mu_{23}) - 2\mu_{12}\mu_{24})}{(\mu_{11} + 2)^2},$$

$$Q_{02} = \frac{\mu_{12}\mu_{14}}{(\mu_{11} + 2)^2}, \quad Q_{01} = \mu_{11} - \frac{\mu_{12}\mu_{21}}{\mu_{11} + 2} + 2$$

$$Q_{10} = -\mu_{12}\mu_{21} - \mu_{11}(\mu_{22} + 2) - 2(\mu_{22} + 2).$$

Next, we assume the following invertible linear transformation:

$$\begin{pmatrix} w \\ z \end{pmatrix} = M \begin{pmatrix} \bar{w} \\ \bar{z} \end{pmatrix}, \quad (13)$$

where

$$M = \begin{pmatrix} 1 + P_{01}(a, b) & 0 \\ -P_{01}(a, b) & 1 \end{pmatrix}.$$

From (12) and (14), it follows that:

$$\begin{pmatrix} \bar{w} \\ \bar{z} \end{pmatrix} \rightarrow \begin{pmatrix} -1 & 1 \\ \omega_1(a, b) & \omega_2(a, b) - 1 \end{pmatrix} \begin{pmatrix} \bar{w} \\ \bar{z} \end{pmatrix} + \begin{pmatrix} f_5(\bar{w}, \bar{z}, a, b) \\ f_6(\bar{w}, \bar{z}, a, b) \end{pmatrix}, \quad (14)$$

where

$$\omega_1(a, b) = Q_{10} + P_{01}Q_{10} - P_{10}Q_{01}, \quad \omega_2(a, b) = P_{10} + Q_{01}$$

$$f_5(\bar{w}, \bar{z}, \alpha, r) = \bar{P}_{20}\bar{w}^2 + \bar{P}_{11}\bar{w}\bar{z} + \bar{P}_{02}\bar{z}^2,$$

$$f_6(\bar{w}, \bar{z}, \alpha, r) = \bar{Q}_{20}\bar{w}^2 + \bar{Q}_{11}\bar{w}\bar{z} + \bar{Q}_{02}\bar{z}^2,$$

$$\bar{P}_{20} = \frac{P_{02}P_{10}^2}{P_{01} + 1} - P_{01}P_{11} + P_{01}P_{20} + P_{20}, \quad \bar{P}_{11} = P_{11} - \frac{2P_{02}P_{10}}{P_{01} + 1},$$

$$\bar{Q}_{11} = P_{10} \left(-\frac{2P_{02}P_{10}}{P_{01} + 1} + P_{11} - 2Q_{02} \right) + (P_{01} + 1)Q_{11}, \quad \bar{P}_{02} = \frac{P_{02}}{P_{01} + 1},$$

$$\bar{Q}_{02} = \frac{P_{02}P_{10}}{P_{01} + 1} + Q_{02},$$

$$\begin{aligned} \bar{Q}_{20} &= (P_1 + 1)^2 Q_{20} + P_{10} (P_1 + 1) (P_{20} - Q_{11}), \\ &+ \frac{P_2 P_{10}^3}{P_1 + 1} + P_{10}^2 (Q_2 - P_{11}). \end{aligned}$$

Taking into account ω_1 and ω_2 , we define the following matrix:

$$\zeta(a_0, b_0) = \begin{pmatrix} \frac{\partial \omega_1}{\partial a}(a_0, b_0) & \frac{\partial \omega_1}{\partial b}(a_0, b_0) \\ \frac{\partial \omega_2}{\partial a}(a_0, b_0) & \frac{\partial \omega_2}{\partial b}(a_0, b_0) \end{pmatrix}.$$

Then by simple calculation $\det \zeta(a_0, b_0)$ is obtained as follows:

$$\det \zeta(a_0, b_0) = -\frac{4s^{3m}}{\Gamma(m+1)^3} \neq 0. \quad (15)$$

Condition (15) is called transversality condition, and it is supposed to be true. Next, we consider $\omega_1(a, b)$ and $\omega_2(a, b)$ for the following parametriza-

tion in the neighborhood of $a = a_0$ and $b = b_0$:

$$\gamma_1 = \omega_1(a, b), \quad \gamma_2 = \omega_2(a, b). \quad (16)$$

Using (16) in (14), we have the following mapping:

$$\begin{pmatrix} \bar{w} \\ \bar{z} \end{pmatrix} \rightarrow \begin{pmatrix} -1 & 1 \\ \gamma_1 & -1 + \gamma_2 \end{pmatrix} \begin{pmatrix} \bar{w} \\ \bar{z} \end{pmatrix} + \begin{pmatrix} f_7(\bar{w}, \bar{z}, \gamma_1, \gamma_2) \\ f_8(\bar{w}, \bar{z}, \gamma_1, \gamma_2) \end{pmatrix}, \quad (17)$$

where

$$f_7(\bar{w}, \bar{z}, \gamma_1, \gamma_2) = g_{20}\bar{w}^2(\gamma_1, \gamma_2) + g_{11}\bar{w}\bar{z}(\gamma_1, \gamma_2) + g_{02}\bar{z}^2(\gamma_1, \gamma_2),$$

$$f_8(\bar{w}, \bar{z}, \gamma_1, \gamma_2) = h_{20}\bar{w}^2(\gamma_1, \gamma_2) + h_{11}\bar{w}\bar{z}(\gamma_1, \gamma_2) + h_{02}\bar{z}(\gamma_1, \gamma_2),$$

$$g_{20}(\gamma, \gamma_2) = \bar{P}_{20}(\gamma, \gamma_2), \quad g_{11}(\gamma, \gamma_2) = \bar{P}_{11}(\gamma, \gamma_2), \quad g_{11}(\gamma, \gamma_2) = \bar{P}_{11}(\gamma, \gamma_2),$$

$$h_{20}(\gamma, \gamma_2) = \bar{Q}_{20}(\gamma, \gamma_2), \quad h_{11}(\gamma, \gamma_2) = \bar{Q}_{11}(\gamma, \gamma_2), \quad h_{02}(\gamma, \gamma_2) = \bar{Q}_{02}(\gamma, \gamma_2).$$

Then, according to Lemma 9.9 [28], p. 437], there exists a near-identity map such that system (14) can be transformed as follows:

$$\begin{pmatrix} x_1 \\ x_2 \end{pmatrix} \rightarrow \begin{pmatrix} -1 & 1 \\ \gamma_1 & -1 + \gamma_2 \end{pmatrix} \begin{pmatrix} z_1 \\ z_2 \end{pmatrix} + \begin{pmatrix} 0 \\ Cz_1^3 + Dz_1z_2 \end{pmatrix} \quad (18) \\ + O(|z_1 + z_2|^4),$$

where

$$C(\gamma_1, \gamma_2) = g_{20}(\gamma_1, \gamma_2)h_{20}(\gamma_1, \gamma_2) + \frac{1}{2}h_{20}^2(\gamma_1, \gamma_2) + \frac{1}{2}h_{20}(\gamma_1, \gamma_2)h_{11}(\gamma_1, \gamma_2),$$

$$\begin{aligned}
D(\gamma_1, \gamma_2) &= \frac{1}{2}g_{20}(\gamma_1, \gamma_2)h_{11}(\gamma_1, \gamma_2) + \frac{5}{4}h_{20}(\gamma_1, \gamma_2)h_{11}(\gamma_1, \gamma_2) \\
&+ h_{20}^2(\gamma_1, \gamma_2) + \frac{1}{2}h_{11}^2(\gamma_1, \gamma_2) + h_{20}(\gamma_1, \gamma_2)h_{02}(\gamma_1, \gamma_2) \\
&+ 3g_{20}^2(\gamma_1, \gamma_2) + \frac{5}{2}g_{20}(\gamma_1, \gamma_2)h_{20}(\gamma_1, \gamma_2) \\
&+ \frac{5}{2}g_{11}(\gamma_1, \gamma_2)h_{20}(\gamma_1, \gamma_2).
\end{aligned}$$

Taking into account theoretical results cited in [28] and the above computations, we have the following result.

Theorem 2. *Assume that $C(0, 0) \neq 0$, $D(0, 0) + 3C(0, 0) \neq 0$, and $\det\zeta(a_0, b_0) \neq 0$, then system (4) experiences 1:2 strong resonance at its positive equilibrium point whenever a and b vary in small neighborhoods of a_0 and b_0 , respectively.*

3.2 1:3 strong resonance

In this subsection, we study codimension-two bifurcation associated with 1:3 strong resonance. For this, assume that a and b are bifurcation parameters. Then characteristic equation of variational matrix of system (4) at (x_*, y_*) has eigenvalues $-\frac{1}{2} \pm \iota \frac{\sqrt{3}}{2}$ if the following condition holds true:

$$\begin{cases} \frac{(b-a)s^m}{(a+b)\Gamma(m+1)} - \frac{(a+b)^2s^m}{\Gamma(m+1)} = -3, \\ s^m \left((a+b)^3s^m - (a^3 + 3a^2b + 3ab^2 + a + b^3 - b) \Gamma(m+1) \right) = 0. \end{cases} \quad (19)$$

We have the following solution of system (19) for a and b :

$$a_1 = \frac{1}{2}\sqrt{3}s^{-3m}\Gamma(m+1) \left(s^{2m} + 3\Gamma(m+1) (s^m - \Gamma(m+1)) \right),$$

$$b_1 = \frac{1}{2}\sqrt{3}s^{-3m}\Gamma(m+1) \left(s^{2m} - 3s^m\Gamma(m+1) + 3\Gamma(m+1)^2 \right).$$

Next, assume that $u_n = x_n - (a+b)$, $v_n = y_n - \frac{b}{(a+b)^2}$ and $a = a_1$ and $b = b_1$, then equilibrium point (x_*, y_*) of (4) is shifted at $(0, 0)$. In this

case (4) transformed into the following map:

$$\begin{pmatrix} u \\ v \end{pmatrix} \rightarrow \begin{pmatrix} \xi_{11} & \xi_{12} \\ \xi_{21} & \xi_{22} \end{pmatrix} \begin{pmatrix} u \\ v \end{pmatrix} + \begin{pmatrix} f_1(u, v) \\ f_2(u, v) \end{pmatrix}, \quad (20)$$

$$\begin{aligned} \xi_{11} &= \frac{(b-a)s^m}{(a+b)\Gamma(m+1)} + 1, & \xi_{12} &= \frac{(a+b)^2 s^m}{\Gamma(m+1)}, \\ \xi_{21} &= -\frac{2bs^m}{(a+b)\Gamma(m+1)}, & \xi_{22} &= 1 - \frac{(a+b)^2 s^m}{\Gamma(m+1)}, \end{aligned}$$

$$\begin{aligned} f_1(u, v) &= r_{11}uv + r_{02}u^2 + O(|u| + |v|)^3, \\ f_2(u, v) &= q_{11}uv + q_{02}u^2 + O(|u| + |v|)^3. \end{aligned}$$

$$\begin{aligned} r_{02} &= \frac{bs^m}{(a+b)^2\Gamma(m+1)}, & r_{11} &= \frac{2(a+b)s^m}{\Gamma(m+1)}, \\ q_{02} &= -\frac{2bs^m}{(a+b)\Gamma(m+1)}, & q_{11} &= -\frac{2(a+b)s^m}{\Gamma(m+1)}. \end{aligned}$$

The eigenvalues of characteristic equation of jacobian matrix of system (20) are $\frac{-1}{2} \pm \frac{\sqrt{3}}{2}i$, let $\rho_1(a_1, b_1)$ and $\varrho_1(a_1, b_1)$ are eigenvector associated with jacobian matrix of (20) and its transpose, respectively and satisfying $\langle \rho_1(a_1, b_1), \varrho_1(a_1, b_1) \rangle = 1$. Then, by simple computation one has;

$$\rho_1(a_1, b_1) = \begin{pmatrix} \frac{1}{-1 + \frac{(3-i\sqrt{3})s^m}{6\Gamma(m+1)}} \\ 1 \end{pmatrix},$$

and

$$\varrho_1(a_1, b_1) = \begin{pmatrix} 1 + \frac{i(\sqrt{3}+3i)s^m}{6\Gamma(m+1)} \\ 1 \end{pmatrix}.$$

Further, any $Y \in \mathbb{R}^2$ can be uniquely described as follows:

$$Y = w\rho_1(a_1, b_1) + \bar{w}\bar{\rho}_1(a_1, b_1), \quad w \in \mathbb{C}.$$

Therefore, the complex form for the map (20) can be written as follows:

$$w \longrightarrow \left(\frac{-1}{2} + \frac{\sqrt{3}}{2} i \right) w + \sum_{2 \leq j+k \leq 3} \frac{1}{j!k!} G_{jk} w^j \bar{w}^k, \quad (21)$$

where

$$\begin{aligned} \bar{G}_{20} &= 3i\sqrt{3}s^{-2m}\Gamma(m+1)^2 - \frac{1}{2}i \left(3\sqrt{3} + (3+3i) \right) s^{-m}\Gamma(m+1) \\ &+ \frac{(3-i\sqrt{3})s^m}{4\sqrt{3}\Gamma(m+1)} + \frac{1}{2}\sqrt{3} \left(1-i\sqrt{3} \right). \end{aligned}$$

$$\begin{aligned} \bar{G}_{11} &= -\frac{ibs^m(s^m-2\Gamma(m+1))(2\sqrt{3}s^m-3i\Gamma(m+1)-3\sqrt{3}\Gamma(m+1))}{\Gamma(m+1)(s^{2m}-3s^m\Gamma(m+1)+3\Gamma(m+1)^2)} \\ &- \frac{ias^m(s^m-2\Gamma(m+1))(2\sqrt{3}s^m-3i\Gamma(m+1)-3\sqrt{3}\Gamma(m+1))}{\Gamma(m+1)(s^{2m}-3s^m\Gamma(m+1)+3\Gamma(m+1)^2)} \\ &+ \frac{6ib\Gamma(m+1)(is^m-\sqrt{3}s^m+2\sqrt{3}\Gamma(m+1))}{(a+b)(s^{2m}-3s^m\Gamma(m+1)+3\Gamma(m+1)^2)} - \frac{2i\sqrt{3}b}{(a+b)^2}. \end{aligned}$$

$$\begin{aligned} \bar{G}_{02} &= \frac{12i(\sqrt{3}+i)as^m(s^{2m}-3s^m\Gamma(m+1)+3\Gamma(m+1)^2)}{\Gamma(m+1)(-3is^m+\sqrt{3}s^m+6i\Gamma(m+1))^2} \\ &+ \frac{12i(\sqrt{3}+i)bs^m(s^{2m}-3s^m\Gamma(m+1)+3\Gamma(m+1)^2)}{\Gamma(m+1)(-3is^m+\sqrt{3}s^m+6i\Gamma(m+1))^2} \\ &+ \frac{36b\Gamma(m+1)(i\sqrt{3}s^m+s^m-2i\sqrt{3}\Gamma(m+1))}{(a+b)(-3is^m+\sqrt{3}s^m+6i\Gamma(m+1))^2} \\ &+ \frac{12i\sqrt{3}b(s^{2m}-3s^m\Gamma(m+1)+3\Gamma(m+1)^2)}{(a+b)^2(-3is^m+\sqrt{3}s^m+6i\Gamma(m+1))^2}. \end{aligned}$$

and $G_{30} = G_{03} = G_{12} = G_{21} = 0$.

Next, according to Lemma 9.12 [[28], p. 448], there exists a smoothly parameter-dependent change of variable such that the map (21) can be

converted into the following form:

$$z \longrightarrow \left(\frac{-1}{2} + \frac{\sqrt{3}}{2} \iota \right) z + F(a_1, b_1) \bar{z} + K(a_1, b_1) z |z|^2 + (|z|^4), \quad (22)$$

where

$$F(a_1, b_1) = \frac{1}{2} G_{02},$$

and

$$K(a_1, b_1) = \left(\frac{1}{2} + \frac{\sqrt{3}}{2} \iota \right) G_{02} G_{11} + \left(\frac{1}{2} + \frac{-1}{2\sqrt{3}} \iota \right) |G_{11}|.$$

Next, we consider the following quantities:

$$F_1(a_1, b_1) = \left(\frac{-3}{2} + \frac{3\sqrt{3}}{2} \iota \right) F(a_1, b_1)$$

$$K_1(a_1, b_1) = -3 |F(a_1, b_1)|^2 - \frac{3}{2} (1 + \sqrt{3} \iota) K(a_1, b_1).$$

Arguing as in Lemma 9.13 [[28], p. 450], we have the following result.

Theorem 3. *Assume that $a = a_1$, $b = b_1$, $ReK_1(a_1, b_1) \neq 0$ and $F(a_1, b_1) \neq 0$, then the system (4) undergoes a 1:3 strong resonance about its fixed point. Moreover, $ReK_1(a_1, b_1)$ determines the stability nature for the bifurcating closed invariant curve.*

3.3 1:4 strong resonance

In this subsection, we study codimension-two bifurcation associated with 1:4 strong resonance. For this, assume that a and b are bifurcation parameters. Then characteristic equation of variational matrix of system (4) at (x_*, y_*) has eigenvalues $\pm \iota$ if the following condition holds true:

$$\begin{cases} \frac{(b-a)s^m}{(a+b)\Gamma(m+1)} - \frac{(a+b)^2 s^m}{\Gamma(m+1)} = -2, \\ s^m ((a+b)^3 s^m - (a^3 + 3a^2b + 3ab^2 + a + b^3 - b) \Gamma(m+1)) = 0. \end{cases} \quad (23)$$

We have the following solution of system (23) for a and b :

$$a_2 = \frac{s^{-3m}\Gamma(m+1)(s^{2m} + 2\Gamma(m+1)(s^m - \Gamma(m+1)))}{\sqrt{2}},$$

$$b_2 = \frac{s^{-3m}\Gamma(m+1)(s^{2m} - 2s^m\Gamma(m+1) + 2\Gamma(m+1)^2)}{\sqrt{2}}.$$

Next, assume that $u_n = x_n - (a+b)$, $v_n = y_n - \frac{b}{(a+b)^2}$ and $a = a_2$ and $b = b_2$, then equilibrium point (x_*, y_*) of (4) is shifted at $(0, 0)$. In this case (4) transformed into the following map:

$$\begin{pmatrix} u \\ v \end{pmatrix} \rightarrow \begin{pmatrix} \theta_{11} & \theta_{12} \\ \theta_{21} & \theta_{22} \end{pmatrix} \begin{pmatrix} u \\ v \end{pmatrix} + \begin{pmatrix} f_3(u, v) \\ f_4(u, v) \end{pmatrix}, \quad (24)$$

$$\theta_{11} = \frac{(b-a)s^m}{(a+b)\Gamma(m+1)} + 1, \quad \theta_{12} = \frac{(a+b)^2 s^m}{\Gamma(m+1)},$$

$$\theta_{21} = -\frac{2bs^m}{(a+b)\Gamma(m+1)}, \quad \theta_{22} = 1 - \frac{(a+b)^2 s^m}{\Gamma(m+1)},$$

$$f_3(u, v) = \chi_{11}uv + \chi_{02}u^2 + O((|u| + |v|)^3),$$

$$f_4(u, v) = \varsigma_{11}uv + \varsigma_{02}u^2 + O((|u| + |v|)^3).$$

$$\chi_{02} = \frac{bs^m}{(a+b)^2\Gamma(m+1)}, \quad \chi_{11} = \frac{2(a+b)s^m}{\Gamma(m+1)},$$

$$\varsigma_{02} = -\frac{bs^m}{(a+b)^2\Gamma(m+1)}, \quad \varsigma_{11} = -\frac{2(a+b)s^m}{\Gamma(m+1)}.$$

The eigenvalues of Jacobian matrix of system (24) are $\pm \iota$, let $p(a_2, b_2)$ and $q(a_2, b_2)$ are eigenvector associated with jacobian matrix of (24) and its transpose, respectively and satisfying $\langle p(a_2, b_2), q(a_2, b_2) \rangle = 1$. Then, by simple computation one has;

$$p(a_2, b_2) = \begin{pmatrix} \frac{(1+i)\Gamma(m+1)}{s^m - (1+i)\Gamma(m+1)} \\ 1 \end{pmatrix},$$

and

$$q(a_2, b_2) = \begin{pmatrix} 1 - \frac{(\frac{1}{2} - \frac{i}{2})s^m}{\Gamma(m+1)} \\ 1 \end{pmatrix}.$$

Moreover, any $Y \in \mathbb{R}^2$ can be described uniquely as follows:

$$Y = wp(a_2, b_2) + \bar{w}\bar{p}(a_2, b_2), \quad w \in \mathcal{C}.$$

Consequently, the complex form for the map (24) can be written as follows:

$$w \longrightarrow (\iota) w + \sum_{2 \leq j+k \leq 3} \frac{1}{j!k!} \bar{G}_{jk} w^j \bar{w}^k, \quad (25)$$

where

$$\begin{aligned} \bar{G}_{20} &= \frac{\frac{(1-i)(a+b)^3 s^m}{\Gamma(m+1)} + \frac{(1+i)b\Gamma(m+1)}{s^m - (1+i)\Gamma(m+1)} + b}{(a+b)^2}, \\ \bar{G}_{11} &= -\frac{2is^m((a+b)^3 s^m + (b - 2(a+b)^3)\Gamma(m+1))}{(a+b)^2\Gamma(m+1)(s^m - (1-i)\Gamma(m+1))}, \\ \bar{G}_{02} &= -\frac{bs^m(s^m - (1+i)\Gamma(m+1))}{(a+b)^2(s^m - (1-i)\Gamma(m+1))^2} \\ &\quad - \frac{(1+i)as^m(s^m - (1+i)\Gamma(m+1))}{\Gamma(m+1)(s^m - (1-i)\Gamma(m+1))} \\ &\quad - \frac{(1+i)bs^m(s^m - (1+i)\Gamma(m+1))}{\Gamma(m+1)(s^m - (1-i)\Gamma(m+1))}, \end{aligned}$$

and $\bar{G}_{30} = \bar{G}_{03} = \bar{G}_{12} = \bar{G}_{21} = 0$.

Next, according to Lemma 9.13 [[28], p. 448], there exists a smoothly parameter-dependent change of variable such that the map (25) can be converted into the following form:

$$z_1 \longrightarrow (\iota) z_1 + F_2(a_2, b_2) z_1 |z_1|^2 + K_2(a_2, b_2) z_1^3 + (|z_1|^4), \quad (26)$$

where

$$F_2(a_2, b_2) = \iota \bar{G}_{11} - \frac{1}{2} \bar{G}_{11} \bar{G}_{20} (1 + \iota) + \bar{G}_{11} \bar{G}_{20} + \bar{G}_{02} \bar{G}_{11} (\iota - 1) - \frac{1}{2} \bar{G}_{11} \bar{G}_{20} (1 - 2\iota),$$

and

$$K_2(a_2, b_2) = \frac{\iota - 1}{4} \bar{G}_{11} \bar{G}_{02} - \frac{\iota + 1}{4} \bar{G}_{11} \bar{G}_{20}.$$

Next, we consider the following quantities:

$$F_3(a_2, b_2) = -4\iota F_2(a_2, b_2)$$

$$K_3(a_2, b_2) = -4\iota K_2(a_2, b_2),$$

whenever $K_3(a_2, b_2) \neq 0$, thus we can write jacobian matrix $J(a_2, b_2) = \frac{F_3(a_2, b_2)}{|K_3(a_2, b_2)|}$. Arguing as in Lemma 9.15 [28], p. 450], we have the following result.

Theorem 4. *Assume that $a = a_2$, $b = b_2$, $ReJ(a_2, b_2) \neq 0$ and $ImJ(a_2, b_2) \neq 0$, then the system (4) undergoes a 1:4 resonance about its fixed point, and $ReJ(a_2, b_2) \neq 0$ determines the stability nature for the bifurcating closed invariant curve.*

4 Numerical simulation

In this section, our main focus is to illustrate theoretical discussion related to codimension-two bifurcation. For this, appropriate parametric values are chosen to discuss emergence of 1:2, 1:3 and 1:4 strong resonances with the help of 3-dimensional bifurcation diagrams and associated maximum Lyapunov exponents (MLE). Mathematica 13.2 is used for this numerical simulation.

Let $a = 1.104600469484825$, $b = 0.817790899566213$, $m = 0.041$, $s = 0.207$, then $(x_*, y_*) = (1.922391369051038, 0.22128840448337964)$. In this case eigenvalue of Jacobian Matrix at (x_*, y_*) is -1 with multiplicity two. Moreover, $det(\zeta(a_0, b_0)) = -\frac{4s^{3m}}{\Gamma(m+1)^3} = -3.52364$, $C(0, 0) = -8.48385$ and $D(0, 0) + 3C(0, 0) = 0.573799$, which shows the correctness of Theorem 2.

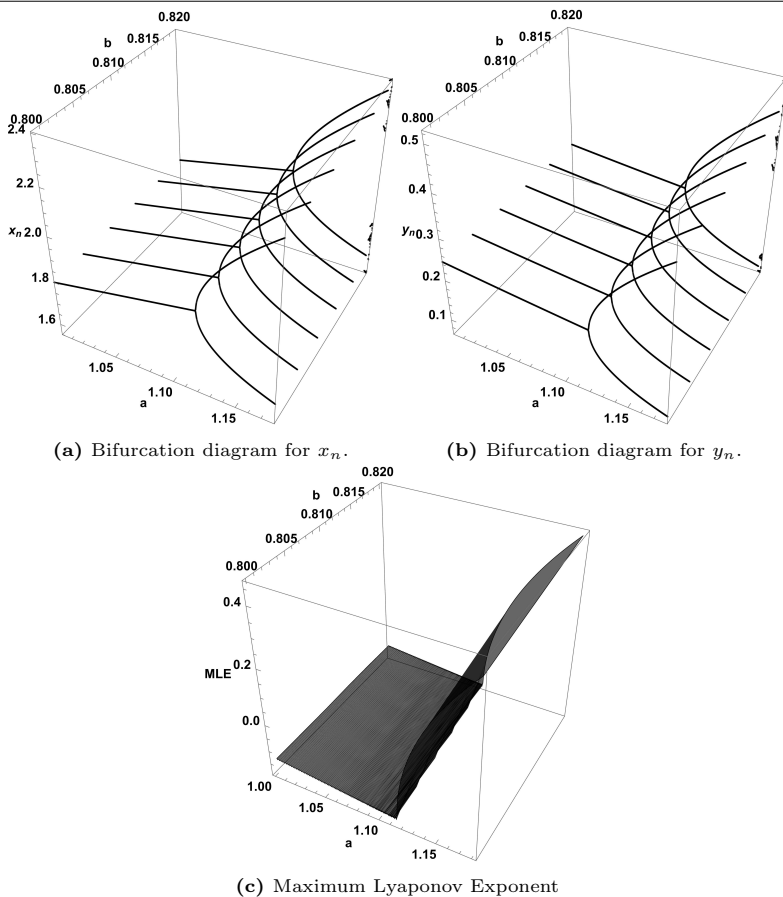
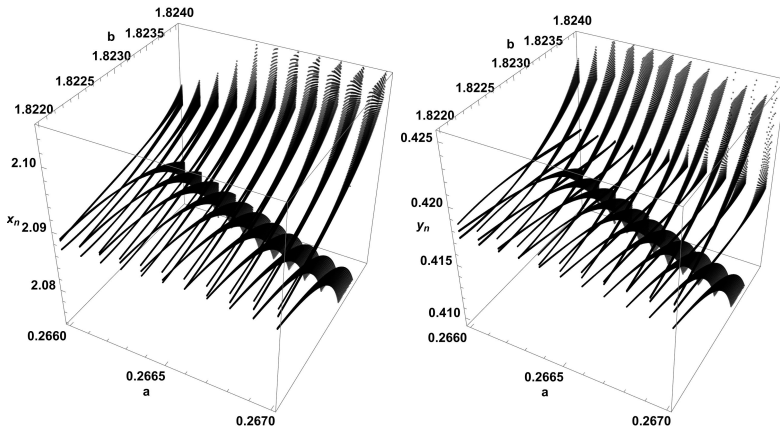


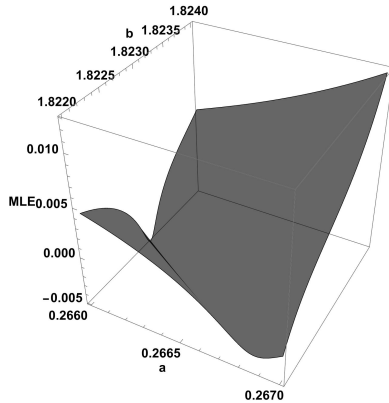
Figure 2. Plots of the system (4) for $m = 0.041$, $s = 0.207$, $a \in [1.001, 1.18]$ and $b \in [0.8, 0.82]$ with initial conditions $x_0 = 1.922$ and $y_0 = 0.221$.

Hence, system (4) undergoes codimension-two bifurcation associated with 1:2 strong resonance whenever $a \in [1.001, 1.18]$ and $b \in [0.8, 0.82]$. Alternatively, the bifurcation diagram in (a, b, x_n) , (a, b, y_n) spaces and MLE are depicted in Figure 2a, 2b and 2c, respectively.



(a) Bifurcation diagram for x_n .

(b) Bifurcation diagram for y_n .

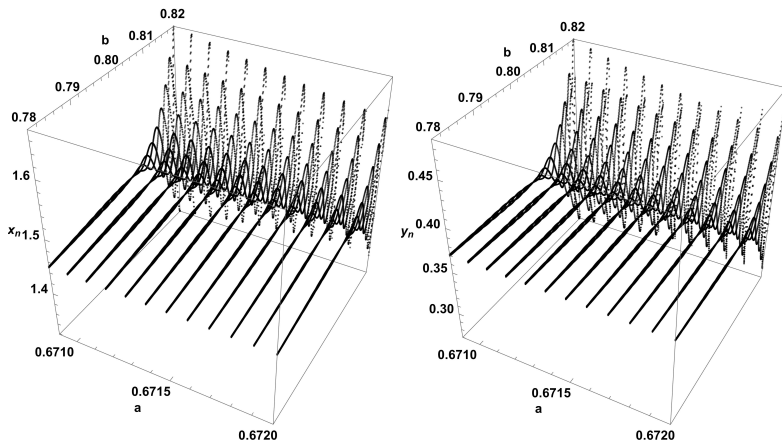


(c) Maximum Lyapunov Exponent

Figure 3. Plots of the system (4) for $m = 0.935$, $s = 0.796$, $a \in [0.266, 0.267]$ and $b \in [1.822, 1.824]$ with initial conditions $x_0 = 2.088$ and $y_0 = 0.4177$.

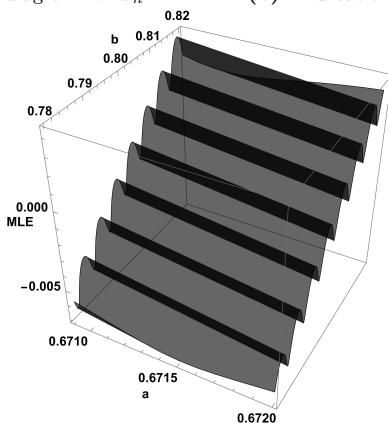
Next, suppose that $a = 0.26642697145189753$, $b = 1.8222532753312775$, $m = 0.935$, $s = 0.796$, then $(x_*, y_*) = (2.088680246783, 0.4177003320148)$. In this case eigenvalues of Jacobian Matrix at (x_*, y_*) are $-\frac{1}{2} \pm i \frac{\sqrt{3}}{2}$. Moreover, $ReK_1(a_1, b_1) = -12.763 \neq 0$ and $F(a_1, b_1) = -0.272546 + 0.2227i \neq 0$, which shows the correctness of Theorem 3. Hence, system (4) undergoes codimension-two bifurcation associated with 1:3 strong resonance whenever $a \in [0.2662, 0.2671]$ and $b \in [1.8221, 1.8224]$. Alternatively, the bifurcation diagram in (a, b, x_n) , (a, b, y_n) spaces and MLE are depicted

in Figure 3a, 3b and 3c, respectively.



(a) Bifurcation diagram for x_n .

(b) Bifurcation diagram for y_n .



(c) Maximum Lyapunov Exponent

Figure 4. Plots of the system (4) for $m = 0.041$, $s = 0.207$, $a \in [0.6709, 0.672]$ and $b \in [0.78, 0.82]$ with initial conditions $x_0 = 1.4752$ and $y_0 = 0.3694$.

Finally, suppose that $a = 0.6711938138764203$, $b = 0.8040745822442753$, $m = 0.041$, $s = 0.207$, then $(x_*, y_*) = (1.4752683961206, 0.36944879641041)$. In this case eigenvalues of Jacobian Matrix at (x_*, y_*) are $\pm \nu$. Moreover, $K_3(a_2, b_2) = 0.902849 + 10.8891\nu$, $Re(J(a_2, b_2)) = 1.0878$ and $Im(J(a_2, b_2)) = 0.569205$, which shows the correctness of Theorem 4. Hence, system (4) undergoes codimension-two bifurcation associated with

1:4 strong resonance whenever $a \in [0.6709, 0.672]$ and $b \in [0.78, 0.82]$. Alternatively, the bifurcation diagram in (a, b, x_n) , (a, b, y_n) spaces and MLE are depicted in Figure 4a, 4b and 4c, respectively.

5 Conclusion

A chemical reaction model is examined for discretization and qualitative analysis. The discrete-time fractional-order Schnakenberg chemical reaction model is derived using the Caputo fractional derivative. It is proven that the system possesses a unique positive equilibrium point. The local dynamics of the model are analyzed, with a focus on determining the parametric conditions required for the local asymptotic stability of the model described in equation (4). Additionally, the discussion includes codimension-two bifurcations. By applying the normal form method and bifurcation theory, it is demonstrated that the fractional-order model described in equation (4) experiences codimension-two bifurcations related to 1:2, 1:3, and 1:4 strong resonances. In the 1:2 resonance scenario, the system displays a resonance pattern in which the frequency of one oscillatory component is twice that of another component. This can cause certain oscillations in the system to be either amplified or suppressed, leading to complex behavior. In the 1:3 resonance situation, the system reveals a resonance pattern where one oscillatory component's frequency is three times that of another component. Much like the 1:2 resonance, this can cause certain oscillations to be either amplified or suppressed, leading to the emergence of complex dynamics. During 1:4 resonance, the system exhibits a resonance pattern in which the frequency of one oscillatory component is four times that of another component. This resonance adds another layer of complexity to the system's dynamics, impacting the amplitudes and phases of different oscillatory components.

Codimension-two bifurcations, including the resonances described earlier, reveal how various oscillatory modes interact and affect one another in the fractional-order Schnakenberg model. The presence of these bifurcations can give rise to complex dynamics, including multiple stable states, chaotic behavior and intricate oscillatory patterns. Analyzing and

describing these codimension-two bifurcations are vital for fully grasping the system's behavior and its effects on chemical reactions and nonlinear dynamics.

In other words, analyzing codimension-two bifurcations in a fractional-order Schnakenberg chemical reaction system can provide insights into the mechanisms and conditions that lead to the emergence of complex dynamics in chemical reactions, as well as offer strategies to control or manipulate these dynamics for practical applications. For example, certain chemical reactions can be utilized to generate signals or patterns for communication or encryption purposes. By adjusting the fractional order or other parameters, it is possible to switch between different modes of operation or improve the system's security and robustness.

Acknowledgment: The authors extend their appreciation to the Deanship of Scientific Research at Northern Border University, Arar, KSA, for funding this research work through the project number NBU-FFR-2024-2230-07.

References

- [1] J. Schnakenberg, Simple chemical reaction systems with limit cycle behavior, *J. Theor. Biol.* **81** (1979) 389–400.
- [2] Q. Din, A novel chaos control strategy for discrete-time Brusselator models, *J. Math. Chem.* **56** (2018) 3045–3075.
- [3] D. L. Benson, J. A. Sherratt, P. K. Maini, Diffusion driven instability in an inhomogeneous domain, *Bull. Math. Biol.* **55** (1993) 365–384.
- [4] L. J. Shaw, J. D. Murray, Analysis of a model for complex skin patterns, *SIAM J. Appl. Math.* **50** (1990) 628–648.
- [5] F. M. Khan, A. Ali, N. Hamadneh, Abdullah, M. N. Alam, Numerical investigation of chemical Schnakenberg mathematical model, *J. Nanomater.* **1** (2021).
- [6] K. S. Noufaey, Semi-analytical solutions of the Schnakenberg model of a reaction-diffusion cell with feedback, *Res. Phys.* **9** (2018) 609–614.

-
- [7] Z. Hammouch, T. Mekkaoui, Numerical simulations for a variable order fractional Schnakenberg model, *AIP Conf.* **1637** (2014) 1450–1455.
- [8] M. Sattari, J. Tuomela, On the numerical simulation of Schnakenberg model on evolving surface, *Math. Sci. Lett.* **4** (2015) 223–234.
- [9] A. Al-Zarka, A. Alagha, S. Timoshin, Transient behaviour in RDA systems of the Schnakenberg type, *J. Math. Chem.* **53** (2015) 111–127.
- [10] F. Yi, E. A. Gaffney, S. Seirin-Lee, The bifurcation analysis of turing pattern formation induced by delay and diffusion in the Schnakenberg system, *Discr. Contin. Dyn. Syst. Ser. B* **22** (2017) 647–668.
- [11] G. Liu, Y. Wang, Pattern formation of a coupled two-cell Schnakenberg model, *Discr. Contin. Dyn. Syst. Ser. S* **10** (2017) 1051–1062.
- [12] P. Liu, J. Shi, Y. Wang, X. Feng, Bifurcations analysis of reaction-diffusion Schnakenberg model, *J. Math. Chem.* **51** (2013) 2001–2019.
- [13] J. Zhu, Y. T. Zhang, S. A. Newman, M. Alber, Application of discontinuous Galerkin methods for reaction–diffusion systems in developmental biology, *J. Sci. Comput.* **40** (2009) 391–418.
- [14] Y. Ishii, K. Kurata, Existence and stability of one-peak symmetric stationary solutions for the Schnakenberg model with heterogeneity, *Discr. Contin. Dyn. Syst. Ser. S* **39** (2019) 2807–2875.
- [15] H. Qian, S. Saffarian, E. L. Elson, Concentration fluctuations in a mesoscopic oscillating chemical reaction system, *Proc. Natl. Acad. Sci. S* **99** (2002) 10376–10381.
- [16] M. VelleLa, H. Qian, On the Poincaré-Hill cycle map of rotational random walk: locating the stochastic limit cycle in a reversible Schnakenberg model, *Proc. R. Soc. A* **466** (2010) 771–788.
- [17] J. D. Murray, *Mathematical Biology*, Springer, New York, 1991.
- [18] A. Goldbeter, *Biochemical Oscillations and Cellular Rhythms: The Molecular Bases of Periodic and Chaotic Behaviour*, Cambridge Univ. Press, London, 1997.
- [19] D. Iron, J. Wei, M. Winter, Stability analysis of Turing patterns generated by the Schnakenberg model, *J. Math. Biol.* **49** (2004) 358–390.

-
- [20] Q. Din, Bifurcation analysis and chaos control in discrete-time glycolysis models, *J. Math. Chem.* **56** (2018) 904–931.
- [21] Q. Din, T. Donchev, D. Kolev, Stability, bifurcation analysis and chaos control in chlorine dioxide/biodine-malonic acid reaction, *MATCH Commun. Math. Comput. Chem.* **79** (2018) 577–606.
- [22] Q. Din, M. A. Iqbal, Bifurcation analysis and chaos control for a discrete-time enzyme model, *Z. Naturforsch. A* **74** (2019) 1–14.
- [23] M. A. Khan, Q. Din, Codimension-one and codimension-two bifurcations of a fractional-order cubic autocatalator chemical reaction system, *MATCH Commun. Math. Comput. Chem.* **91** (2024) 415–452.
- [24] M. Y. Ongun, D. Arslan, J. Farzi, Numerical solutions of fractional order autocatalytic chemical reaction model, *Süleyman Demirel Univ. Fen Bilim. Enst. Derg.* **21** (2017) 165–172.
- [25] Q. Din, K. Haider, Discretization, bifurcation analysis and chaos control for Schnakenberg model, *J. Math. Chem.* **58** (2020) 1615–1649.
- [26] Q. Din, Controlling chaos and codimension-two bifurcation in a discrete fractional-order Brusselator model, *J. Vib. Control.* in press. <https://doi.org/10.1177/10775463241267033>
- [27] M. J. Uddin, M. S. Rana, Chaotic dynamics of the fractional order Schnakenberg model and its control, *Math. App. Sci. Eng.* **4** (2023) 40–60.
- [28] Y. A. Kuznetsov, *Elements of Applied Bifurcation Theory*, Springer, New York, 2004.
- [29] Y. Yang, Q. Qi, J. Hu, J. Dai, C. Yang, Adaptive fault-tolerant control for consensus of nonlinear fractional-order multi-agent systems with diffusion, *Fractal Fract.* **10** (2023) #760.
- [30] T. Jia, X. Chen, L. He, F. Zhao, J. Qiu, Finite-time synchronization of uncertain fractional-order delayed memristive neural networks via adaptive sliding mode control and its application, *Fractal Fract.* **10** (2022) #502.
- [31] Y. Zhao, Y. Sun, Z. Liu, Y. Wang, Solvability for boundary value problems of nonlinear fractional differential equations with mixed perturbations of the second type, *AIMS Math.* **1** (2020) 557–567.

-
- [32] R. Xing, M. Xiao, Y. Zhang, J. Qiu, Stability and Hopf bifurcation analysis of an $(n+m)$ -neuron double-ring neural network model with multiple time delays, *J. Sys. Sci. Complex.* **35** (2022) 159–178.
- [33] C. Xu, Y. Zhao, J. Lin, Y. Pang, Z. Liu, J. Shen, Y. Qin, Bifurcation investigation and control scheme of fractional neural networks owning multiple delays, *J. Comput. Appl. Math.* **43** (2024) 1–33.
- [34] C. Xu, M. Farman, A. Shehzad, K. Sooppy Nisar, Modeling and Ulam-Hyers stability analysis of oleic acid epoxidation by using a fractional-order kinetic model, *Math. Methods Appl. Sci.* in press. <https://doi.org/10.1002/mma.10510>
- [35] Q. Din, U. Saeed, Stability, discretization, and bifurcation analysis for a chemical reaction system, *MATCH Commun. Math. Comput. Chem.* **90** (2023) 151–174.
- [36] Q. Din, Dynamics and Hopf bifurcation of a chaotic chemical reaction model, *MATCH Commun. Math. Comput. Chem.* **88** (2022) 351–369.
- [37] Q. Din, M. S. Shabbir, M. A. Khan, A cubic autocatalator chemical reaction model with limit cycle analysis and consistency preserving discretization, *MATCH Commun. Math. Comput. Chem.* **87** (2022) 441–462.